ELSEVIER

Polymer 44 (2003) 2689–2699

polymer

www.elsevier.com/locate/polymer

In situ monitoring of reaction-induced phase separation with modulated temperature DSC: comparison between high-T_g and low-T_g modifiers

Steven Swier, Bruno Van Mele*

Faculty of Applied Sciences, Department of Physical Chemistry and Polymer Science-FYSC (TW), Vrije Universiteit Brussel-VUB, Pleinlaan 2, B-1050 Brussels, Belgium

Received 26 September 2002; received in revised form 31 January 2003; accepted 5 February 2003

Abstract

A linearly polymerizing and network forming epoxy–amine system will be modified with high-T_g thermoplastics poly(ether sulphone) (PES: $T_g = 223$ °C) and poly(ether imide) (PEI: $T_g = 210$ °C) and with a low-T_g copolymer poly(ethylene oxide)-block-poly(propylene oxide)-block-poly(ethylene oxide) (triblock: $T_g = -70$ °C). Both PES and the triblock show lower critical solution temperature (LCST)-type demixing behavior, while PEI exhibits upper critical solution temperature (UCST)-type demixing with epoxy resins. Reaction-induced phase separation (RIPS) in these modified systems is studied using Modulated Temperature DSC (MTDSC) as an in situ tool. The thermoplastic-rich phase of the high-T_g modifier will vitrify at some point, while that of the low-T_g modifier stays mobile during curing at the useful curing temperatures, affecting the diffusion rates of the epoxy–amine species in (to) this phase differently. By using the heat capacity signal during quasi-isothermal cure, phase separation can be measured indirectly as a step-wise decrease due to vitrification of the thermoplastic-rich phase or directly as a peak when the heat of phase separation occurs on the time-scale of the modulation. The latter effect has been detected for the first time with MTDSC in the case of RIPS. Temperature-conversion-transformation diagrams unambiguously show the LCST-type demixing behavior of these systems, while information about the in situ developed morphology can be obtained from the heat capacity evolutions in non-isothermal post-cures.

Keywords: Modulated temperature differential scanning calorimetry; Reaction-induced phase separation; Thermoset cure

1. Introduction

In recent years a lot of progress has been made in developing multi-component, reactive epoxy–amine systems in order to achieve heterogeneous structures with tailor-made properties. To improve the impact resistance of inherently brittle epoxy resins, for example, toughening with rubber particles has been commonly used in the past [1]. To avoid deterioration of other mechanical properties such as the elastic modulus and yield stress, these low-T_g modifiers can be substituted with high-T_g engineering thermoplastics like poly(ether sulphone) (PES) and poly-(ether imide) (PEI) [2,3]. The common principle used to achieve these heterogeneous epoxy resins consists of curing an initially homogeneous three-component mixture, which results in an increase in molecular weight of the epoxy–amine, therefore initiating phase separation at a certain conversion [4]. The low starting viscosity of the reactive mixture allows for easy processing through, for example, casting and resin transfer molding. Reaction-induced phase separation (RIPS) is the result of a decrease in the entropic contribution to the free energy of mixing during polymerization [2]. The increase in conversion leads to a 'chemical quench' from the miscible to the immiscible region of the phase diagram by either a decrease of the lower critical solution temperature (LCST: case of PES) or an increase of the upper critical solution temperature (UCST: case of PEI) [5–10]. Depending on the composition of the quasi-binary blend, the material will enter the metastable or unstable region during this process, in principle resulting in the nucleation and growth or spinodal decomposition mechanism, respectively, [11]. However, especially in the case of high-T_g modifiers, thermodynamics is merely the driving force for phase separation, while the kinetics of interdiffusion between the coexisting phases will become

* Corresponding author. Tel.: +32-2-629-32-76/88; fax: +32-2-629-32-78.

E-mail address: bvmele@vub.ac.be (B. Van Mele).

0032-3861/03/$ - see front matter © 2003 Elsevier Science Ltd. All rights reserved.
doi:10.1016/S0032-3861(03)00138-1

determining at some point [12,13]. Crucial in this respect is the ratio between the rate of phase separation and that of chemical reaction. For a certain modifier chemistry and composition, the cure temperature (T_{cure}) will be the most important parameter influencing both rates at the same time [14]. The interdependence of these rates reveals the complexity in controlling the morphology in these systems. An increase in T_{cure} in a system showing LCST type demixing behavior, for example, will, together with the resulting lower conversion at phase separation (x_{ps}), increase the interdiffusion rates at x_{ps}. However, the corresponding higher cure rate also results in a faster molecular weight increase of the epoxy–amine beyond this point, reducing the diffusion rate of the components in the reactive mixture. Additional points of interest are the gel point of the epoxy–amine and possible vitrification of either of the coexisting phases. The former corresponds to the onset of network formation of the epoxy–amine rich phase. While the composition of different phases will further evolve after gelation and a secondary phase separation may also be initiated [2], the development of the primary morphology is possibly arrested at the gel point [15]. The latter occurs in the case where T_{cure} is below the full cure glass transition of either the epoxy–amine rich phase, $T_{g\ full}$, or the modifier-rich phase, $T_{g\ MOD}$. Vitrification can fix the morphology at a certain conversion, thus freezing in a thermodynamically unstable polymer system. An example was given by Poncet, where the high glass transition of the poly(phenylene ether) phase inhibited the epoxy–amine species from diffusing, thus fixing the morphology of the continuous phase [16]. While the aforementioned modifiers usually exist as phases in the micrometer range, there is considerable recent interest in designing nanostructured materials as well [17,18]. In this case a solution containing an amphiphilic compound like the copolymer poly(ethylene oxide)-block-poly(propylene oxide) and a reactive compound self-assembles to form a nano-scale structure, which is unchanged during the course of cure and is subsequently fixed at full cure.

To clarify these aspects, Gillham proposed cure diagrams to optimize processing and material properties of epoxy resins [19]. By including the onset of phase separation, the succession of chemical and physical events during isothermal RIPS can be predicted [20,21]. These time–temperature–transformation (TTT) and time–conversion–transformation (TxT) diagrams have to be used with caution, since, in principle, the two phases originating at the cloud point have their own cure diagrams. Thus, cure diagrams can be used to pinpoint the crucial events during RIPS, but adequate control over the morphology requires a measuring technique capable of studying the evolution of chemorheology in situ. Modulated Temperature DSC (MTDSC) has the potential to measure both the reaction advancement and effects of rheological changes in one experiment with excellent temperature control [22,23]. This was illustrated for PES-modified epoxy–amine systems, for which RIPS can be detected indirectly as a step-wise decrease of the heat capacity due to vitrification of the segregating PES-rich phase [23]. If cure is performed sufficiently below $T_{g\ full}$, both vitrification of the PES-rich phase and vitrification of the epoxy-rich phase can be observed. While the cloud point itself cannot be detected with MTDSC in RIPS of the PES-modified epoxy–amines, another study looking at temperature-induced phase separation in poly(ethylene oxide)/PES shows that the onset in the evolution of the heat capacity with temperature exactly corresponds to the cloud point as measured by optical microscopy [24,25]. Heat effects associated with demixing and remixing, which occur on the time-scale of the modulation, cause this excess contribution in the heat capacity signal, therefore designated apparent heat capacity. The principal objective of this paper is to extend the analysis of RIPS with MTDSC to both high-T_g and low-T_g modifiers using different epoxy-based systems as reactive components. Optical microscopy data will be combined with MTDSC measurements, which provide in situ information on cure advancement (heat flow signal) and chemorheological effects (heat capacity signal). The focus will be on modifiers that ultimately form a micro-scale structure.

2. Experimental

2.1. Materials

Two epoxy–amine systems were studied: a bifunctional epoxy, diglycidyl ether of bisphenol A (DGEBA, Epon825 from Shell), with an epoxy equivalent weight (EEW) of 180 g equiv.$^{-1}$, in combination with an appropriate amount of a bifunctional amine (aniline from Fluka), or a tetrafunctional amine hardener (methylene dianiline, MDA from Janssen Chimica), with amine equivalent weights of 46.5 and 49.5 g equiv.$^{-1}$, respectively. Different mixtures of these pure systems were prepared with 20 and 50 wt% of poly(ether sulphone) (PES from Aldrich: $M_w = 20,000 \times$ g mol^{-1}; $T_g = 223$ °C) and of the triblock copolymer poly(ethylene oxide)-block-poly(propylene oxide)-block-poly(ethylene oxide) (from Aldrich: $M_n = 4400$ g mol^{-1} with 30 wt% ethylene oxide; $T_g = -70$ °C). No distinction in T_g could be made between the poly(ethylene oxide) and poly(propylene oxide) blocks in the copolymer. Literature data for the homopolymers, however, reveal that the T_g of poly(propylene oxide) (−75.2 °C [26]) is 8 °C lower than that of poly(ethylene oxide) (67.2 °C [26]). Crystallization of poly(ethylene oxide) and the copolymer is difficult to avoid in quench experiments and might influence the measured T_g values, which therefore only serve as an indication for the fully amorphous material.

To obtain a homogeneous mixture of the high-T_g modified DGEBA + aniline, PES was first dissolved in the epoxy using CH_2Cl_2, which was evaporated at about 120 °C under extensive stirring followed by vacuum

evaporation at 100 °C. Aniline was mixed afterwards for about 5 min at 80 °C. For the network system, the appropriate quantities of all components (DGEBA + MDA/PES) were dissolved in CH_2Cl_2/CH_3OH (99/1), followed by solvent evaporation at 40 and 80 °C under vacuum for 1 h and 5 min, respectively. The DGEBA + MDA/triblock system was mixed at 80 °C for 5 min. All these preparation methods reduce the amount of preliminary reaction to a minimum.

DGEBA (LY556 from Vantico, EEW = 188.5 g equiv.^{1}) was used in the DGEBA + MCDEA/PEI system. The amine curing agent was 4,4′-methylenebis(3-chloro-2,6-diethylaniline) (MCDEA from Aldrich, $M_w = 380$ g mol^{-1}). The thermoplastic modifier was poly(ether imide) (PEI, Ultem 1000 from General Electric, $M_n = 26,000$ g mol^{-1}). The blending procedure for DGEBA + MCDEA/PEI was as in Ref. [27].

2.2. Techniques

Cure experiments were performed on a TA Instruments 2920 DSC with MDSC™ option and a Refrigerated Cooling System (RCS). Helium was used as a purge gas (25 ml min^{1}). Indium and cyclohexane were used for temperature calibration. The former was also used for enthalpy calibration. Heat capacity calibration was performed with a PMMA standard (supplied by Acros) using the heat capacity difference between two temperatures, one above and one below the glass transition temperature of PMMA [26], to make sure that heat capacity changes were adequately measured. Cure was performed in hermetic aluminum pans (TA Instruments) with sample weights between 5 and 10 mg. Modulation conditions were: amplitude of 1 °C and a 60 s period. Non-isothermal post-cures and final (second) heatings were usually conducted at 2.5 °C min^{-1} up to 240 °C. Cloud points were detected by measuring the light transmitted through thin samples (held between glass slides) in a Mettler Toledo FP82HT hot stage equipped with a photodetector. A Spectratech optical microscope was used with a magnification of 4. When the cloud point could not be measured with optical microscopy, a Perkin–Elmer Lambda 40 UV/Vis spectrometer was used in the visible (VIS) spectral range with the same hot stage set-up.

3. Results and discussion

3.1. Indirect determination of RIPS: vitrification of modifier-rich phase

3.1.1. PES-modified epoxy–amines

3.1.1.1. Time–conversion–transformation (TxT) diagram for DGEBA + aniline/20 wt%PES. RIPS in the epoxy–amine systems DGEBA + aniline and DGEBA + MDA, modified with the high-T_g engineering thermoplastic PES, can be probed as vitrification of the PES-rich phase [22,23]. The former system modified with 20 wt% PES is shown at three cure temperatures in Fig. 1. The non-reversing heat flow and the initial increase in the heat capacity signal contain complementary information on the epoxy–amine reaction [22,28]. The decrease in the heat capacity signal accompanied by a relaxation peak in the heat flow phase marks the time at which the T_g of the PES-rich phase (T_g pure PES = 223 °C) rises above the cure temperature and the mobility of this phase is frozen in. In case the cure temperature is below the full cure glass transition of the epoxy–amine ($T_{g\ full} = 95$ °C), vitrification of the segregating phase rich in this component can also take place. This clearly occurs in Fig. 1 for the reaction at 80 °C. The heat flow phase is important in this respect, clearly showing a second relaxation peak. Only partial vitrification is seen at 90 °C, and it is again most obvious in the heat flow phase. Upon curing an unmodified epoxy–amine in a temperature range corresponding to the glass transition region of the fully cured system, this effect of partial vitrification was also seen [22]. It indicates that a fraction of the material remains

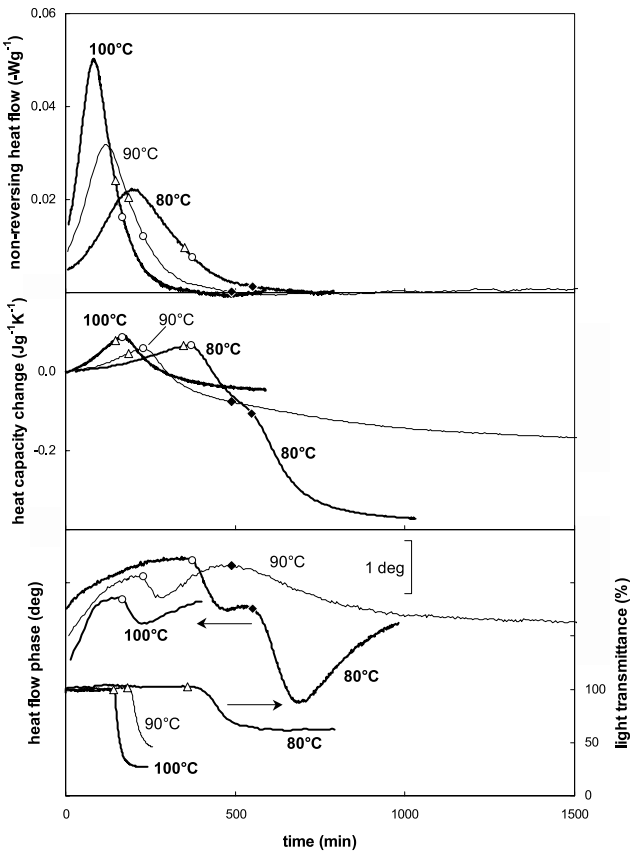

Fig. 1. Non-reversing heat flow, change in heat capacity and heat flow phase signal from MTDSC and % of light transmittance from optical microscopy (OM) for the reactive blend DGEBA(Epon825) + aniline ($r = 1$)/20 wt%PES cured at 100, 90 and 80 °C; the cloud point from OM (△), onset of heat flow phase relaxation corresponding to vitrification of PES-rich phase (○) and epoxy–amine-rich phase (◆) are shown and also indicated in the heat flow and heat capacity signals.

mobile on the time-scale of the modulation. An increase in modulation frequency or decrease in temperature would induce further vitrification.

The fact that RIPS is not measured directly with MTDSC in this system can be inferred from light transmittance experiments, also performed at 80, 90 and 100 °C in Fig. 1: the onset of phase separation (cloud point) obtained in this way (△) occurs prior to the onset of vitrification of the PES-rich phase calculated from the heat flow phase (○). The latter signal is also used to pinpoint the vitrification of the epoxy–amine rich phase (◆).

Partial integration of the non-reversing heat flow signal gives the epoxy conversion corresponding to the three major events discussed in Fig. 1. A wide range of cure temperatures (60–155 °C) was studied in this way to construct the temperature–conversion–transformation (TxT) diagram of the DGEBA + aniline system modified with 20 wt% PES (Fig. 2). Cure temperatures higher than 140 °C were measured without modulation to decrease the equilibration time for these fast cures. Therefore, only the cloud point conversion could be calculated. The negative slope of this curve (△) holds proof of the LCST-type demixing behavior of this system: for a higher cure temperature the onset of phase separation will be encountered at lower conversions [2,4,14]. For comparison, the network-forming system DGEBA + MDA, modified with 20 wt% PES, exhibits phase separation at 41% conversion at 100 °C (66% for DGEBA + aniline, Fig. 2), prior to the gelation point at 58% conversion [29]. This network system's LCST is thus lower and/or its cloud point curve is broader at lower conversions resulting in a stronger tendency to phase separate.

The vitrification line of the epoxy–amine-rich phase has also been included in Fig. 2 (◆) and reflects the expected T_g–x behavior [19]. Further phase separation accompanied by morphology changes will be inhibited beyond this point. This line is also shown for the unmodified epoxy–amine system (×) and matches that of the modified system, meaning that the epoxy–amine-rich phase contains little or no PES. Otherwise, the high-T_g component would increase the glass transition of this phase and decrease the conversion at which vitrification sets in.

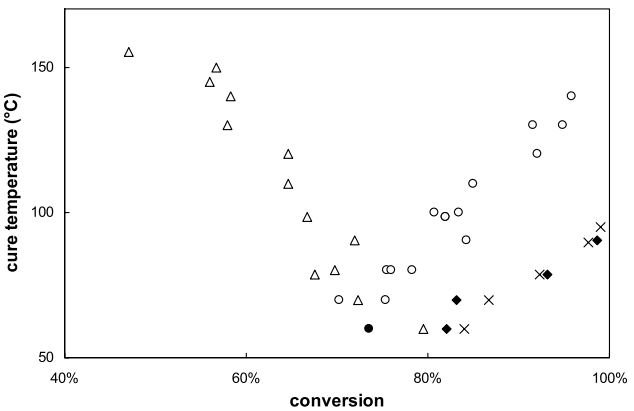

Fig. 2. TxT diagram for a stoichiometric DGEBA(Epon825) + aniline/20 wt%PES mixture with: cloud points from optical microscopy (△), onset of heat flow phase relaxation corresponding to vitrification of PES-rich phase (○) and epoxy–amine-rich phase (◆); the cloud point at 60 °C was obtained by using UV/Vis spectrometry in transmittance at 450 nm; vitrification of the homogeneous mixture at 60 °C (●); the onset in the heat flow phase relaxation corresponding to vitrification of the pure DGEBA(Epon825) + aniline ($r = 1$) is given for reference (×).

In case a pure PES-phase would be formed at phase separation, vitrification of this phase would occur immediately in the range of cure temperatures studied (60–155 °C), resulting in a coinciding cloud point curve and vitrification line of this PES-phase. This is obviously not the case (Fig. 2). In contrast to the cloud point curve, a positive slope is also found for the vitrification line of the PES-rich phase (○). This can be understood by realizing that the T_g of this phase is determined by its composition and by the T_g of its constituents. At higher cure temperatures, vitrification occurs for a phase richer in PES. This means that the cloud point curve will have decreased more to achieve purer coexisting phases in comparison to lower cure temperatures.

While this information could also be obtained from the combination of dynamic rheometry or dynamic mechanical analysis, which provide the onset of vitrification, and DSC, which provides the conversion [30], the advantage of using one technique (MTDSC) with excellent temperature control that can measure both is evident. By using the complementary techniques, the TxT diagram of an epoxy–amine system modified with PEI was obtained, where an UCST-type demixing behavior was observed [20]. In this case both the cloud point curve and the vitrification curve were found to exhibit a positive slope, characteristic of UCST-type demixing behavior.

The combination of an almost pure epoxy–amine-rich phase and a PES-rich phase changing in composition reveals the asymmetry of the phase diagram: one branch will be close to the pure epoxy–amine, while the other branch will gradually evolve to purer PES as temperature and conversion rises. This asymmetry has also been simulated within the framework of the Flory–Huggins theory and is related to the difference in molecular weight between PES and the epoxy resin [10]. Phase diagrams constructed for mixtures of DGEBA and PES with different molecular weights also confirm this idea [5,31]. Moreover, non-isothermal experiments after isothermal cure above $T_{g\,full}$ have already shown that the epoxy–amine rich phase does not attain a glass transition higher than 95 °C [23]. Curing at higher temperatures just results in a higher fraction of this phase.

It should be noted, however, that the reaction mechanism can be altered when the modifier is added and during RIPS [32,33]. This would result in a change in the vitrification line in comparison to the unmodified case. A scenario could be pictured in which the epoxy–amine has a lower T_g at the same conversion due to a change in reaction mechanism, compensated with a certain amount of PES present in the epoxy–amine rich phase. While this is rather unlikely, it cannot be excluded a priori and would also result in

coinciding vitrification lines for the unmodified and modified case.

A remark has to be made here about RIPS at low cure temperatures (< 80 °C) also included in the TxT diagram of Fig. 2. The cloud point and vitrification line of the PES-rich phase evidently cross at some low cure temperature where both the onset of phase separation and the vitrification of the PES-rich phase coincide (around 70 °C). At 60 °C, however, the onset of vitrification of this phase seems to occur prior to the detection of the cloud point. Note that since no decrease in light transmittance was seen in optical microscopy for this temperature, UV/Vis spectroscopy was used here in transmittance at a wavelength of 450 nm, still capable of detecting the cloud point. This probably indicates that the phases formed at the cloud point are too small to be detected by the optical technique. Still, vitrification of the PES-rich phase prior to the cloud point seems unlikely.

A possible explanation could be that no phase separation (and thus no vitrification of a PES-rich phase) but merely vitrification of the homogeneous system occurs at this point (Fig. 1, ● at 60 °C). More information can be obtained by looking at the change in heat capacity at 60 °C and, especially, the derivative of the heat capacity signal to time as a function of conversion (Fig. 3). Indeed, while the proposed TxT diagram is essential to control reactive blends with appropriate precuring and postcuring schedules, more information is present about the time-dependency of phase separation and morphology development in the MTDSC experiment itself. The unmodified system in Fig. 3 shows one step-wise decrease in C_p corresponding to vitrification of the epoxy–amine matrix, while a double decrease in C_p is seen for the modified system. Beyond vitrification of the homogeneous modified system (●), a diffusion-controlled cure takes place, which induces phase separation (△) after a long cure time (over 16 h). At this cloud point (△: 79% conversion), the glass transition of a pure DGEBA + aniline phase would be 50 °C (obtained from the $T_g x$ relation). This (epoxy-rich) phase might therefore devitrify partially at 60 °C and will revitrify after further reaction. Vitrification of the co-existing PES-rich phase will occur faster due to its higher T_g, which shows up as an acceleration of vitrification and a second peak in the derivative of C_p.

If the cure temperatures would be decreased even further (below 60 °C), a homogeneous mixture will vitrify completely, impeding the occurrence of phase separation.

3.1.1.2. Network forming DGEBA + MDA/50 wt%PES: Effect of reactive mixture composition. When epoxy–amine network systems are cured with higher thermoplastic contents, sudden reactivity increases are found at phase separation [34,35]. This can be seen in the DGEBA + MDA ($T_{g\ full}$ = 175 °C for r = 1) system, modified with 50 wt% PES in Fig. 4. In case a stoichiometric mixture of the epoxy–amine is used (①), RIPS results in a shoulder (indicated by the arrow) in the non-reversing heat flow

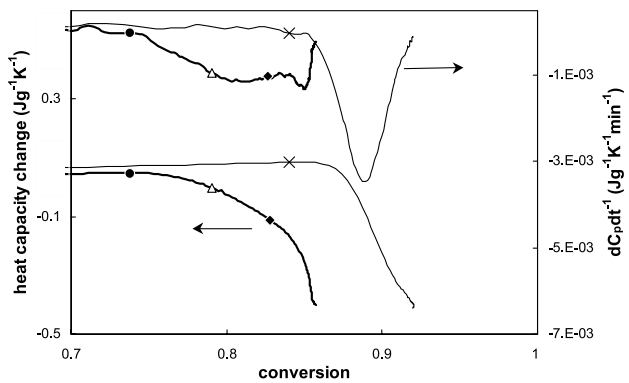

Fig. 3. Change in heat capacity and derivative of the heat capacity signal to time as a function of the reaction conversion (determined from the non-reversing heat flow) for the unmodified (thin line) and 20 wt% PES modified (thick line) stoichiometric DGEBA(Epon825) + aniline system at 60 °C; the cloud point as detected by UV/Vis spectroscopy is also included (△), other symbols are as in Fig. 2.

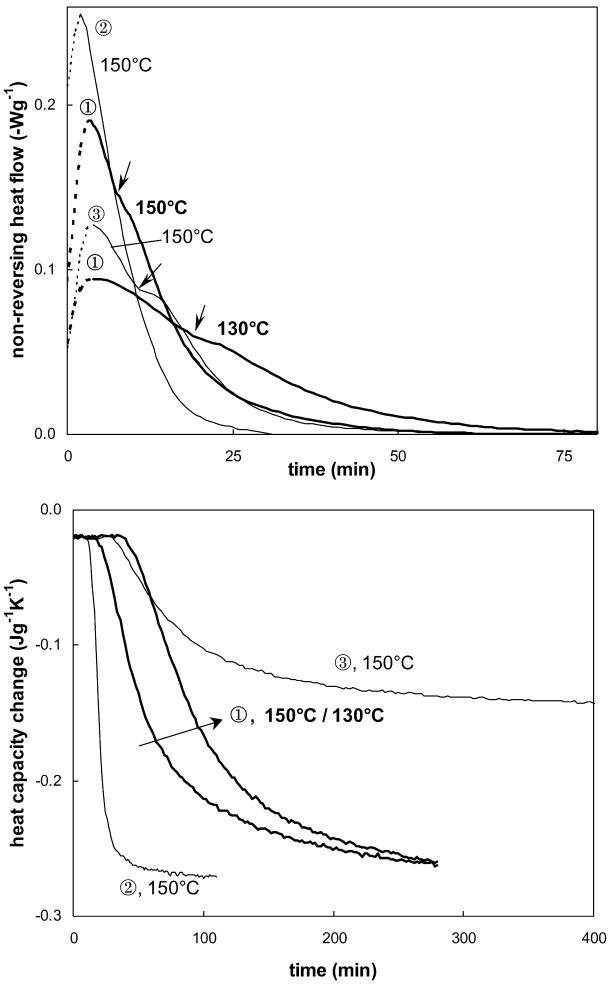

Fig. 4. Non-reversing heat flow and change in heat capacity (note the longer time scale) for the reactive blend DGEBA(Epon825) + MDA/50 wt%PES: stoichiometric mixtures of the epoxy–amine are cured at 150 and 130 °C (r = 1: ①); an excess amine (r = 1.4: ②) and excess epoxy (r = 0.7: ③) mixture is cured at 150 °C; dashed line corresponds to the time the sample temperature needs to reach the cure temperature within 0.5 °C; arrows indicate onset of shoulder in non-reversing heat flow (see text).

signal after 7 and 20 min for T_{cure} equaling 150 and 130 °C, respectively. Note that high cure temperatures had to be used here to induce phase separation at low enough conversions. Otherwise, vitrification of the relatively high-T_g homogeneous reactive blend occurs prior to the cloud point, and no RIPS can be seen (not shown). This can be compared with the effects noticed in Fig. 1 for the DGEBA + aniline system at a lower T_{cure} (60 °C). The disadvantage of using these high cure temperatures is, however, that the first collected data points are unreliable (dashed line in Fig. 4). Instead of using different cure temperatures, the rate of reaction and phase separation can be changed more independently by using different mixture compositions for the reactive epoxy–amine component. This only holds in the case that the change in epoxy–amine ratio alters the reaction rate but does not affect the position and shape of the cloud point curve too much resulting in a similar driving force at the onset of phase separation. Three mixture compositions of DGEBA + MDA, all cured at 150 °C, are shown in Fig. 4. A decrease in reactivity is seen in the order: excess amine ($r = 1.4$, ②), stoichiometric mixture ($r = 1$, ①) and excess epoxy ($r = 0.7$, ③). The shoulder in the non-reversing heat flow, indicating a reactivity increase accompanying RIPS, is not present in the first mixture.

As introduced in the previous section, the simultaneous heat capacity information contains additional chemorheological information (see also Fig. 1). The change in heat capacity, however, does not exhibit the double step-wise decrease in any of the studied compositions. The fact that the glass transitions of both phases are close together could be responsible for this insensitivity in the stoichiometric system (see Table 1), which was already discussed for the same epoxy–amine modified with 20 wt% PES [23]. On the other hand, the lower glass transitions of both off-stoichiometric systems (Table 1) means that no vitrification of a pure epoxy–amine phase can occur.

The total decrease in heat capacity as seen in Fig. 4 is related to the amount of material that has vitrified during the isothermal cure step at, for example, 150 °C. When the heat capacity changes (ΔC_p) between the glassy and the rubbery or liquid state are known for both the epoxy–amine and the thermoplastic at T_{cure}, the fraction of vitrified material can be obtained. This fraction can be estimated by taking the heat capacity change at T_g equal to T_{cure} for the epoxy–amine systems and by extrapolating the evolutions of the heat capacity above and below the T_g for PES (Table 1). For the stoichiometric system with 50 wt% PES, this corresponds to vitrifying almost all the material in the mixture. In case of the excess epoxy system, a close correspondence is found with vitrification of the PES phase only (Table 1: compare 0.12 with 0.27 divided by 2). When the excess amine is used, however, the decrease in heat capacity is more than what would be expected for the PES phase alone. This therefore indicates vitrification of a homogeneous, partially reacted mixture of epoxy–amine and PES having a higher glass transition in comparison to the unmodified system.

To clarify the isothermally obtained information, Fig. 5 depicts the derivative of the heat capacity signal as a function of temperature for different preceding cure schedules. Calculation of heat capacity changes at T_g of

Table 1
Heat capacity changes measured in isothermal and non-isothermal conditions for the unmodified and modified DGEBA(Epon825) + MDA($r = 1$)/PES system

Unmodified						
	DGEBA + MDA			PES		
r: NH/epoxy	0.7	1	1.4			
ΔC_p (T_{gfull})	0.40 (91)	0.27 (175)	0.32 (137)	0.21 (223)[a]		
ΔC_p at 150 °C	n.a.[b]	0.31[c]	n.a.[b]	0.27[d]		
50% PES modified						
	DGEBA + MDA-rich phase			PES-rich phase		
r: NH/epoxy	0.7	1	1.4	0.7	1	1.4
ΔC_p during cure at 150 °C[e]	0.12	0.24	0.21			
Non-isothermal ΔC_p (T_g)[f] obtained after						
Iso 150 °C	0.19 (113)	0.09 (160)	0.27 (172)[g]	0.14 (163)	0.15 (173)	
Iso 150 °C + iso 230 °C	0.18 (115)	0.14 (170)	0.13 (155)	0.09 (188)	0.07 (196)	0.12 (174)
N-i at 10 °C min^{-1} to 230 °C	0.18 (117)	0.16 (164)	0.17 (137)	0.13 (194)	0.08 (222)	0.09 (210)

[a] ΔC_p is given at the T_g of PES.
[b] T_{gfull} is below 150 °C for these systems.
[c] From experimental ΔC_p vs. T_g curve for DGEBA + MDA.
[d] Extrapolation of ΔC_p from 223 to 150 °C.
[e] Total decrease in C_p is given from Fig. 4: no distinction can be made between coexisting phases.
[f] Overlapping peaks from $dC_p\ dT^{-1}$ during post-cure experiments were deconvoluted using Gaussian functions [36].
[g] Total integration of $dC_p\ dT^{-1}$ is given for this homogeneous material.

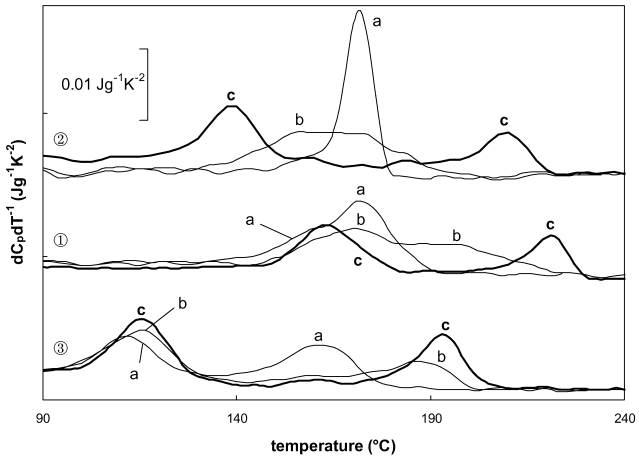

Fig. 5. Derivative of heat capacity to temperature ($dC_p dT^{-1}$) for non-isothermal post-cure measurements at 2.5 °C min^{-1} following: isothermal cure at 150 °C (see Fig. 4) (a); isothermal cure at 150 °C followed by post-cure at 230 °C for 30 min (b) and non-isothermal cure at 10 °C min^{-1} to 230 °C (c); studied systems: stoichiometric ($r = 1$: ①), excess amine ($r = 1.4$: ②) and excess epoxy ($r = 0.7$: ③) DGEBA(Epon825) + MDA/50 wt%PES; $T_{g\ full}$ equals 175, 137 and 91 °C for $r = 1$, 1.4 and 0.7, respectively, (see Table 1).

the high-T_g and low-T_g phases obtained from integration of these curves are also given in Table 1. This method was first proposed to study interphase behavior in interpenetrating polymer networks [36,37]. After the isothermal cure of the stoichiometric system at 150 °C (a, ①) this signal has a maximum at 173 °C with a shoulder about 10 °C lower, indicating two phases with similar glass transitions and a significant amount of interpenetration. Thus, while DGEBA + MDA/PES has a stronger thermodynamic driving force to phase separate as compared to the linear system (previous section), slow diffusion probably dictates the phase separation. To initiate phase separation at a lower conversion, thus increasing diffusion rates, cure can be performed non-isothermally at a high heating rate (c, ①). It is clear that this method results in a better segregation of the coexisting phases and points out the diffusion rate as the rate-determining step. Another issue which is frequently addressed in literature is that the network fixes the morphology therefore freezing in a thermodynamically unstable system [2,5]. This can be easily shown here by adding a post-cure step at 230 °C to the system which was isothermally cured at 150 °C and measuring the resulting thermal properties (b, ①). While a better separation of both T_g's is achieved after this post-cure step (see also Table 1), the system does not attain the segregation of the non-isothermal cure. Thus looking at the derivative of the heat capacity signal can be useful in the design of cure schedules to achieve a desired end material in view of interphase and morphology. As indicated, curing at lower temperatures increases the amount of interphase, which corresponds to a decrease in 'particle size' [38].

For the excess amine system, the non-isothermal post-cure experiment in Fig. 5 after the isothermal cure at 150 °C only shows one glass transition at 172 °C (a, ②) corresponding to the absence of phase separation as envisioned before. The higher reactivity seen in Fig. 1 can be held responsible for a reduction in the time available for the development of phase separation. Indeed, the lower T_g of this excess amine system (137 °C, see Table 1) would result in higher diffusion rates in comparison to the stoichiometric system (175 °C) and would increase this time. By applying the non-isothermal cure step, phase separation can be initiated at a higher temperature (c, ②) and thus lower conversion, resulting in higher diffusion rates. The high-T_g and low-T_g phases are clearly separated with values close to the pure phases (see also Table 1).

For the excess epoxy system, a much lower glass transition in combination with the lower reactivity will result in higher diffusion rates and more time for morphology evolution at 150 °C. The resulting marked segregation is translated into two distinct glass transitions already seen after the isothermal cure at 150 °C (a, ③). Note that while a $T_{g\ EPAM}$ (113 °C) higher than $T_{g\ full}$ (91 °C) is found (probably due to residual PES) no vitrification of this phase can occur at 150 °C. Other cure schedules (non-isothermal at 10 °C min^{-1} and post-cure at 230 °C after cure at 150 °C) are also shown. The fact that both schedules result in similar end properties for the excess epoxy means that further interdiffusion to attain the thermodynamically stable end state is less restricted than in the other mixtures. The lower crosslink density of this system could be responsible for this effect [39].

3.1.2. PEI-modified epoxy–amine

When poly(ether imide) (PEI: $T_g = 210\ °C$) is added to epoxy–amine systems, upper critical solution temperature (UCST) type demixing behavior is found [3]. Adding this component to DGEBA + MDA, however, does not result in phase separation since MDA is considered to be too reactive to allow interdiffusion to occur before vitrification [40]. Therefore lower reactive amines like diamino diphenyl sulphone (DDS) or 4,4-methylene bis(3-chloro-2,6-diethylamine) (MCDEA) should be used and have been studied extensively in the past [20,33,34,41]. A few aspects are reviewed in this work to illustrate the added value of MTDSC, especially regarding slowly reacting systems [42]. The isothermal cure at 138 °C is shown for a stoichiometric mixture of DGEBA + MCDEA modified with 45 wt% of PEI in Fig. 6. Since peak-to-peak noise in the non-reversing heat flow is 30 μW over 1000 min, this signal cannot be considered to be reliable to measure the low reaction rate isothermally in this system (also compare scale of non-reversing heat flow of Fig. 6 with those of Fig. 1 and Fig. 4). The heat capacity and heat flow phase in this slowly reacting system, however, both clearly show that RIPS occurs, with a good separation in time (conversion) of both vitrification events. The low conversion at the onset of phase separation

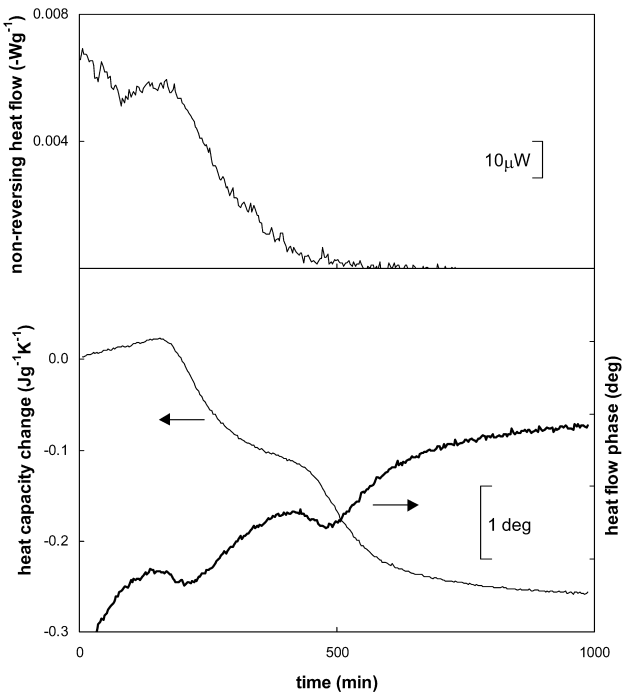

Fig. 6. Non-reversing heat flow, change in heat capacity and heat flow phase signal for the cure of the reactive mixture DGEBA(LY556) + MCDEA/45%PEI ($r = 1$) at 138 °C.

is responsible for this effect, as confirmed by both light scattering and SAXS measurements [20,34].

Fig. 7 shows the effect of cure schedule on the thermal properties of the heterogeneous system formed during reaction. A better separation is again seen after the additional non-isothermal post-cure step in comparison to that seen after only the isothermal cure (thin line). Morphological analysis has shown that phase separation induced at higher cure temperatures in this system indeed results in larger particles with less interphase, corresponding to a larger separation in glass transitions [41]. Since the network structure after isothermal cure restricts the amount of segregation, performing a non-isothermal cure directly on

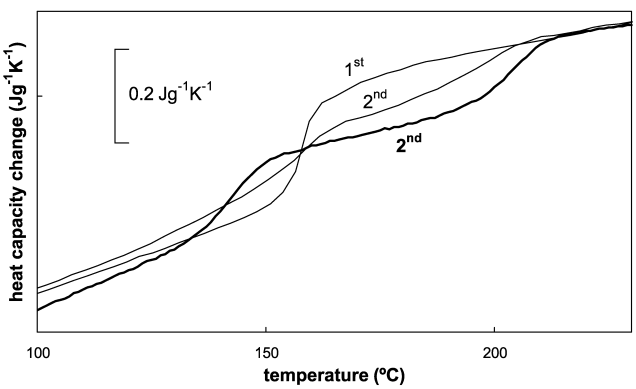

Fig. 7. Heat capacity signal during a non-isothermal post-cure measurement (at 2.5 °C min^{-1}): after the isothermal cure at 138 °C (depicted in Fig. 6) (first and second heating, thin line) and after a non-isothermal cure at 1 °C min^{-1} (second heating, thick line).

an unreacted sample (thick line) shows an even larger separation as confirmed by a morphological study [41].

3.2. Direct determination of RIPS: excess contribution in heat capacity signal

Both the vitrification seen in the heat capacity signal of the PES-rich phase and the shoulder in the non-reversing heat flow corresponding to a reactivity increase are indirect probes for RIPS. While the heat of demixing can be obtained by conventional DSC to determine the onset of temperature-induced phase separation in partially miscible polymer blends [43], the simultaneous occurrence of the much larger reaction enthalpy in RIPS dominates the heat flow signal. Miscibility gaps in non-reactive, low and high molecular weight blends have been constructed by using DSC, although poorly resolved signals are obtained that are difficult to interpret [43–46]. MTDSC, and in particular the heat capacity signal, proves to be useful for determining the cloud point temperature associated with phase separation in polymer blends showing LCST behavior [24]. This signal is termed ‘apparent heat capacity’ in this case since excess contributions arising from heat effects of demixing and remixing on the time-scale of the modulation are retrieved. Since noise and baseline effects turn up in the non-reversing heat flow and not in the heat capacity signal, small heat effects related to phase separation in polymer blends can still be measured (less than 2 J g^{-1} for PEO/PES). Moreover, the (apparent) heat capacity can also be followed quasi-isothermally allowing the real-time study of the kinetics of demixing and remixing in isothermal conditions for different blend compositions and molecular weights of the components [25].

When this methodology is extended to RIPS, simultaneous reaction and phase separation could be envisioned to be deconvoluted in the non-reversing heat flow and the heat capacity signal, respectively. Since the modified epoxy systems as discussed above did not show any heat effects related to phase separation in the heat capacity signal, this either means that phase separation was too slow to occur on the time scale of the modulation or too much spread out in time to be distinguished from noise or both. Increasing the interdiffusion rates by avoiding vitrification of the thermoplastic-rich phase is a possible route to increasing the rate of phase separation considerably [34]. In this work, the low-T_g poly(ethylene oxide)-block-poly(propylene oxide)-block-poly(ethylene oxide) copolymer (designated ‘triblock’: $T_g = -70$ °C) is used in combination with the DGEBA + MDA network system. A propylene oxide fraction of 70 wt% makes sure that phase separation is induced in the micrometer range [17,47] as is the case in the aforementioned systems. When lower fractions of this component or other amphiphilic modifiers are used, nano-phase self-assembly results in the formation of nano-structured materials, while mixing is seen on the micrometer range over the entire conversion range [18,47,48]. The marked

influence of the type and amount of a certain block arises from the fact that the poly(propylene oxide) block becomes immiscible with epoxy–amines at a certain x, while the poly(ethylene oxide) block has been stated to be miscible throughout cure [17,47,49].

Isothermal cure at temperatures from 50 to 120 °C is shown in Figs. 8 and 9 for 20 and 50 wt% of the triblock component, respectively. Although the presence of the triblock copolymer significantly lowers the viscosity of the reactive mixture, the reaction rate of this mixture is not higher than that of the PES-modified one prior to phase separation. On the contrary, for the cure at 80 °C, the PES-modified system is actually the more reactive of both 20 wt% modified systems (showing a more pronounced auto-acceleration in Fig. 8). If the rheology of the reacting systems would influence the reaction rate and diffusion-controlled reaction would interfere, the opposite effect would be expected. A mechanistic model for the chemically-controlled reaction kinetics reveals that the difference in reaction rate actually results from the amount of specific hydrogen-bonding interactions between the modifier and the epoxy–amine species [50].

For the low-T_g modifier no vitrification of the phase rich in this component is expected. The step-wise decrease in heat capacity actually sets in when the T_g of the epoxy–amine rich phase rises above the cure temperature. Phase separation together with cure of this phase has to occur to achieve this T_g rise. Indeed, no vitrification is detected when

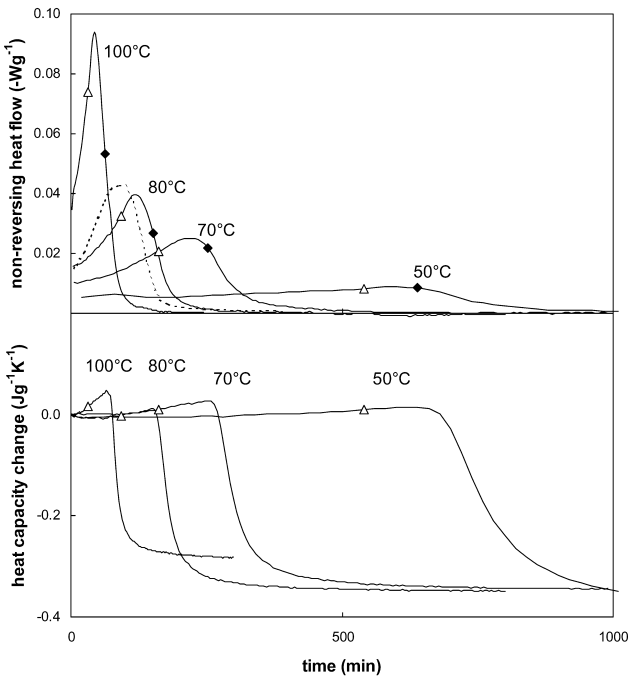

Fig. 8. Non-reversing heat flow and change in heat capacity for the cure of the reactive mixture DGEBA + MDA/20 wt% triblock (PEO_PPO_PEO) ($r = 1$) at 50, 70, 80 and 100 °C; the cure of DGEBA + MDA/20 wt%PES at 80 °C is given for comparison (— — —); cloud points from OM (△) and onsets of heat flow phase relaxation corresponding to vitrification of the epoxy–amine-rich phase (◆) are also indicated.

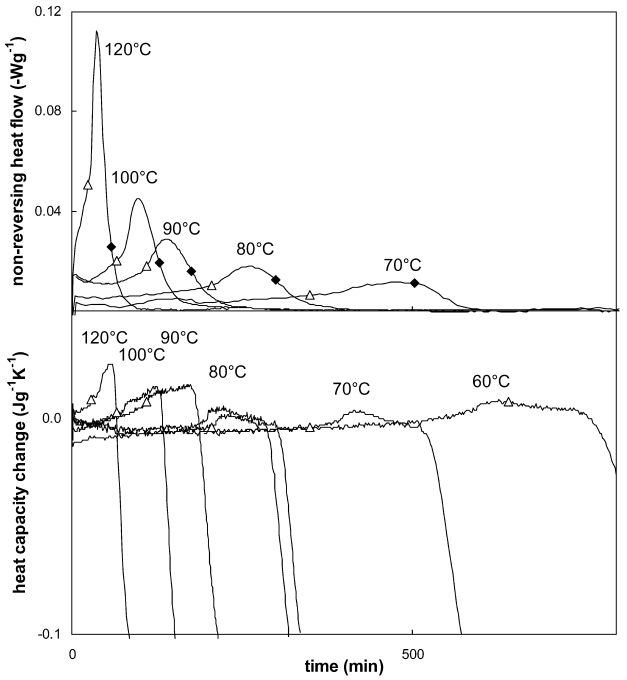

Fig. 9. Non-reversing heat flow and change in heat capacity for the cure of the reactive mixture DGEBA + MDA/50 wt% triblock ($r = 1$) at 60, 70, 80 (C_p reproduced), 90, 100 and 120 °C; cloud points from OM (△) and onsets of heat flow phase relaxation corresponding to vitrification of the epoxy–amine-rich phase (◆) are also indicated.

a random poly(ethylene oxide)-co-poly(propylene oxide) modifier with a much higher fraction of PEO (75 wt%) is used as modifier for DGEBA + MDA, since RIPS does not take place for this system (not shown).

The focus here will lie on the region around the onset of phase separation. Cloud points obtained by optical microscopy are indicated on the MTDSC signals (△). This point marks the onset of a reactivity increase in the non-reversing heat flow especially for the 50 wt% triblock system. The higher concentration of reactive groups in the still mobile epoxy–amine phase is responsible for this effect. While the PES-modified system in Fig. 1 also exhibits this effect, a much lower conversion at phase separation magnifies the effect for the triblock system. Slower interdiffusion rates in the high-T_g modified system could also smear out this 'concentration effect' in time. In the heat capacity signal an additional peak can be seen for the 50 wt% triblock system having its onset close to the cloud point. This effect is superimposed upon the increase in heat capacity due to chemical reaction.

The TxT diagram is constructed in Fig. 10 including the cloud points from optical microscopy, the onsets of phase separation from the heat capacity of MTDSC (for the 50 wt% triblock) and the vitrification line of the epoxy–amine rich phase. Again the negative slope for the onsets of phase separation confirms the LCST-type demixing behavior while the positive slope of the vitrification line corresponds to the expected T_g–x behavior. The conversion at the cloud point for the 20 wt% system is consistently

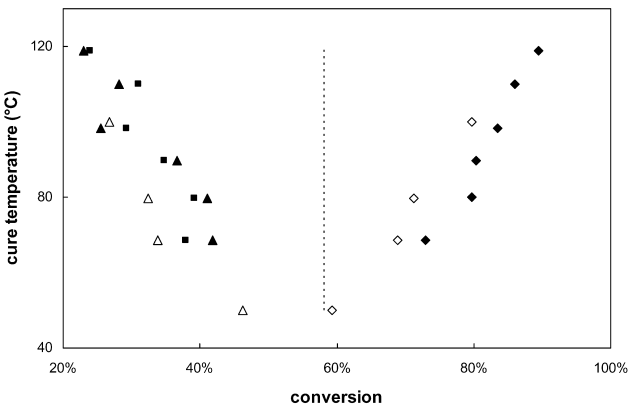

Fig. 10. TxT diagram for stoichiometric DGEBA + MDA mixtures modified with 20 and 50 wt% triblock; cloud points from optical microscopy (20 wt%: △, 50 wt%: ▲) and the onsets of the heat flow phase relaxation corresponding to vitrification of the epoxy–amine-rich phase (20 wt%: ◇, 50 wt%: ◆) are shown; the onset of the peak in the apparent heat capacity is also included (50 wt%: (■); the conversion at gelation (58%) is indicated (– – –) [29].

lower than that for the 50 wt% one. This might indicate that the critical point of the phase diagram lies lower than 20 wt% triblock at the onset of phase separation. A similar conclusion was drawn in the case of poly(2,6-dimethyl-1,4-phenylene ether) (PPE) exhibiting UCST-type demixing behavior with epoxy resins by using conventional DSC together with light scattering data [51]. A comparable difference between both modifier concentrations is seen for the vitrification line and is related to the lower T_g of the epoxy–amine rich phase for the higher modifier content.

The nice correspondence between the cloud points by OM and the onset of phase separation by MTDSC confirms the origin of the peak in the apparent heat capacity. As envisioned in the introduction of this section, heat effects associated with phase separation on the time scale of the modulation are probably responsible for this peak. To support this further an estimation is made for the total heat that is exchanged by integrating the excess contribution from the raw modulated heat flow. In this way, a value of 1.5 J g^{-1} for the total heat effect at 80 °C is obtained. This corresponds to values found for temperature-induced phase separation in polymer blend systems [24,52]. Thus, for low-T_g modifiers like the triblock copolymer, isothermal RIPS could be measured for the first time directly and quantitatively with MTDSC.

4. Conclusions

The TxT diagram of RIPS in the linearly polymerizing DGEBA + aniline modified with 20 wt% PES can be constructed by using MTDSC in conjunction with optical microscopy. This diagram can be used to design appropriate cure schedules. Vitrification times of both the high-T_g PES-rich phase and the low-T_g epoxy-rich phase can be obtained in quasi-isothermal conditions from step-wise decreases in the heat capacity signal, while the corresponding conversions are calculated from the simultaneous non-reversing heat flow information. The cloud point exhibits a negative slope thus confirming the LCST-type demixing behavior. A positive slope is found for the vitrification line of the PES-rich phase, which corresponds to the relation between its composition/glass transition and the cure temperature. Vitrification lines for the low-T_g phase and the unmodified epoxy–amine coincide and are indicative of an asymmetric phase diagram with one branch close to the pure epoxy–amine component.

Both the time-dependency of phase separation and the morphology advancement influence the evolution in the heat capacity signal. This is further illustrated in the network forming system DGEBA + MDA/50 wt% PES where the amount of material that freezes in during RIPS can be estimated. When the amine is used in excess ($T_{g\ full}$ = 137 °C), more material is found to freeze in at 150 °C than the fraction expected in case only the PES-rich phase would vitrify. This is related to the high reactivity of this system, which does not allow enough time for phase separation to occur. Thus, vitrification of a (higher T_g) homogeneous reactive blend takes place. Lower reactivities are found for the stoichiometric and excess epoxy mixtures (also cured at 150 °C) where the non-reversing heat flow does show a reactivity increase indicating a concentration effect of reactive groups at RIPS. The derivative of the heat capacity signal in non-isothermal post-cure experiments confirms these findings and can also be used to study the effect of cure temperature on the final morphology, in particular the interphase development.

The in situ study of RIPS with MTDSC can be extended by introducing PEI as a high-T_g modifier in the epoxy–amine DGEBA + MCDEA exhibiting UCST-type demixing behavior. While the reaction cannot be measured quantitatively in the non-reversing heat flow for this low-reactive system, the double step-wise decrease in the heat capacity signal clearly indicates phase separation for this system. The lower conversion at the cloud point together with the larger T_g difference between the coexisting phases is responsible for this effect. Both MTDSC signals of non-isothermal post-cure experiments confirm these statements.

Using a low-T_g triblock copolymer instead of the high-T_g PES to modify DGEBA + MDA did not result in a reactivity increase prior to the onset of phase separation since T_{cure} is sufficiently above the T_g of the homogeneous system at this point. When phase separation sets in, a clear reactivity increase is seen, especially for the 50 wt% triblock system. The higher interdiffusion rates beyond this point also result in an additional excess contribution in the heat capacity in quasi-isothermal conditions. Since the onset of this effect corresponds well with the cloud point for different cure temperatures, the ‘apparent’ heat capacity signal can be used as a direct probe for RIPS in this system.

The TxT diagram again holds evidence for an LCST-type

demixing behavior and shows that only the epoxy–amine rich phase vitrifies after a certain conversion. A first attempt is made to quantify the heat effect associated with phase separation using the excess heat capacity contribution.

Acknowledgements

The work of S. Swier was supported by grants of the Flemish Institute for the Promotion of Scientific-Technological Research in Industry (I.W.T.).

References

[1] Kinloch AJ. Adv Polym Sci 1985;72:45.
[2] Williams RJJ, Rozenberg BA, Pascault JP. Adv Polym Sci 1997;95:128.
[3] Hodgkin JH, Simon GP, Varley RJ. Polym Adv Technol 1998;9:3.
[4] Inoue T. Prog Polym Sci 1995;20:119.
[5] Yamanaka K, Inoue T. Polymer 1989;30:622.
[6] Riccardi CC, Borrajo J, Williams RJJ, Girard-Reydet E, Sautereau H, Pascault JP. J Polym Sci: Part B 1996;34:349.
[7] Jansen BJP, Meijer HEH, Lemstra PJ. Polymer 1999;40:2917.
[8] Yamanaka K, Takagi Y, Inoue T. Polymer 1989;60:1839.
[9] de Graaf LA, Hempenius MA, Möller M. Polym Prepr 1995;36:787.
[10] Clarke N, McLeish TCB, Jenkins SD. Macromolecules 1995;28:4650.
[11] MacKnight WJ, Karasz FE. Polymer characterization. In: Allen G, Bevington JC, editors. Polymer blends. Comprehensive polymer science, vol. 1. Oxford: Pergamon Press; 1989. p. 113–30.
[12] Kiefer J, Hilborn JG, Hedrick JL. Polymer 1996;37:5715.
[13] Rajagopalan G, Gillespie JW, McKnight SH. Polymer 2000;41:7723.
[14] Tran-Cong Q, Shibayama M. In: Araki T, editor. Structure and properties of multiphase polymeric materials. Marcel Dekker; 1998.
[15] Kim BS, Chiba T, Inoue T. Polymer 1993;34:2809.
[16] Poncet S, Boiteaux G, Pascault JP, Sautereau H, Seytre G, Rogozinski J, Kranbuehl D. Polymer 1999;40:6811.
[17] Mijovic J, Shen M, Wing Sy J. Macromolecules 2000;33:5235.
[18] Lipic PM, Bates FS, Hillmyer MA. J Am Chem Soc 1998;120:8963.
[19] Gillham JK, Enns JB. Trends Polym Sci 1994;2:406.
[20] Girard-Reydet E, Vicard V, Pascault JP, Sautereau H. J Appl Polym Sci 1997;65:2433.
[21] Boogh L, Pettersson B, Månson J-A. Polymer 1999;40:2249.
[22] Swier S, Van Assche G, Van Hemelrijck A, Rahier H, Verdonck E, Van Mele B. J Therm Anal 1998;54:585.
[23] Swier S, Van Mele B. Thermochim Acta 1999;330:175.
[24] Dreezen G, Groeninckx G, Swier S, Van Mele B. Polymer 2001;42:1449.
[25] Swier S, Pieters R, Van Mele B. Polymer 2002;43:3611.
[26] Gaur U, Wunderlich B. J Phys Chem Ref Data 1982;11:313. ATHAS database on the World Wide Web: web.utk.edu/ ~ athas/databank/intro.html.
[27] Bonnet A, Pascault JP, Sautereau H, Camberlin Y. Macromolecules 1999;32:8524.
[28] Swier S, Van Mele B, submitted for publication.
[29] Younes M, Wartewig S, Lellinger D, Strehmel B, Strehmel V. Polymer 1994;35:5269.
[30] Ishii Y, Ryan AJ. Macromolecules 2000;33:167.
[31] Bucknall CB, Gomez CM, Quintard I. Polymer 1994;35:353.
[32] Mondragon I, Corcuera MA, Martin MD, Valea A, Franco M, Bellenguer V. Polym Int 1998;47:152.
[33] Bonnaud L, Pascault JP, Sautereau H. Eur Polym J 2000;36:1313.
[34] Bonnet A, Pascault JP, Sautereau H, Taha M, Camberlin Y. Macromolecules 1999;32:8517.
[35] Ritzenthaler S, Girard-Reydet E, Pascault JP. Polymer 2000;41:6375.
[36] Hourston DJ, Song M, Schafer F-U, Pollock HM, Hammiche A. Polymer 1999;40:4769.
[37] Hourston DJ, Song M, Pollock HM, Hammiche A. J Therm Anal 1997;49:209.
[38] Martinez I, Martin MD, Eceiza A, Oyanguren P, Mondragon I. Polymer 2000;41:1027.
[39] Oleinik EF. Adv Polym Sci 1986;80:49.
[40] Siddhamalli SK. Polym-Plastics Technol Engng 2000;39:699.
[41] Girard-Reydet E, Sautereau H, Pascault JP, Keates P, Navard P, Thollet G, Vigier G. Polymer 1998;39:2269.
[42] Van Mele B, Rahier H, Van Assche G, Swier S. The application of MTDSC for the characterization of curing systems. In: Reading M, editor. The characterization of polymers using advanced calorimetric methods. Kluwer Academic Publishers; 2003. in press.
[43] Arnauts J, De Cooman R, Vandeweerdt P, Koningsveld R, Berghmans H. Thermochim Acta 1994;238:1.
[44] Shen S, Torkelson JM. Macromolecules 1992;25:721.
[45] Natansohn A. J Polym Sci: Part C 1985;23:305.
[46] Ebert M, Garbella RW, Wendorff JH. Makromol Chem, Rapid Commun 1986;7:65.
[47] Guo Q, Thomann R, Gronski W, Thurn-Albrecht T. Macromolecules 2002;35:3133.
[48] Hillmyer MA, Lipic PM, Hadjduk DA, Almdal K, Bates FS. J Am Chem Soc 1997;119:2749.
[49] Zheng S, Zhang N, Luo X, Ma D. Polymer 1995;36:3609.
[50] Swier S, Van Mele B, submitted for publication.
[51] Ishii Y, Ryan AJ. Macromolecules 2000;33:158.
[52] Moore JA, Kim JH. Macromolecules 1992;25:1427.